



ALGORITHMS FOR PROCESSING MEDICAL GRAPHIC IMAGES FOR UTERINE FIBROID SEGMENTATION

Aripova Zulfiya Dilshodovna

Tashkent University of Information Technologies

Email: mezulik@gmail.com

Actuality

Segmentation methods became popular in image processing and analysis. Fibroid segmentation from Ultrasound Image is a complex problem in the field of medical imaging. Fibroids are Non Cancerous tumors, which grow in Female body. Sinologists use the technique called Ultrasonography, to solve diagnostic problems such as identifying the abnormal tissues or fibroids. They routinely use ultrasound information to develop an image. But images contain noise with maculation that leads to poor image quality.

Keywords: Dynamic model, Shape statistical model, Active contour, ultrasound image segmentation, Uterine fibroid

Introduction

The development and introduction of information technologies and computer technology has led to the emergence of new methods and tools for diagnostics and visualization. The doctor has new opportunities to purposefully influence the process of visualization of a medical image for high-quality diagnostics. Currently, the doctor, depending on the type of examination, often needs to independently determine image processing algorithm, and for this he needs to provide tools that allow carry out such processing in the shortest possible time. The capabilities of modern computers and graphic visualization tools make it possible to satisfy almost any request related to the processing of medical images, and a workstation with software and hardware for processing and visualizing medical images can serve as a tool for making a diagnosis [1].

Main Part

Medical research based on modern imaging techniques allows look inside the objects of a living organism and diagnose its condition. The solution of this problem involves a number of stages of image processing in order to analyze and recognize objects. Formation of images in various devices and their further transmission through different channels provoke distortion, so the first stage of image processing is filtering





or eliminating low-frequency noise. This stage allows us to distinguish the objects of interest to us from all others and from the background. Analysis of publications shows that the most effective in practical terms are additive Gaussian and impulse noise models. Additive Gaussian noise is characterized by adding values from corresponding normal distribution with zero mean. Such noise appears in digital imaging devices. Impulse noise is characterized by the replacement of some pixels by fixed or random values. This noise is associated with losses in the transmission of images over communication channels. In a real image, you can find both additive and impulse noise, such noise called combined. All types of filters can be divided into classes: frequency, linear, non-linear, combined, hybrid and adaptive. The choice of filter depends on the characteristics of the image and noise [2]. The stages following the filtering involve the use of image processing methods such as segmentation, selection of area boundaries. Each processing method is based on the use some numerical characteristics of the image and their functional features [3]. Segmentation is related to the division of the image into areas for which a certain homogeneity criterion, for example, highlighting areas of approximately the same brightness in the image. The concept of an image area is used to define a coherent group of image elements that have a certain common attribute (property). One of the main and simple ways is to build a segmentation using a threshold. The threshold is a sign (property) that helps to divide the desired signal into classes. The threshold division operation is to compare the brightness value of each pixel images with a given threshold value. Let us present a block diagram of a segmentation algorithm based on difference of "zero" levels of wavelet transforms.

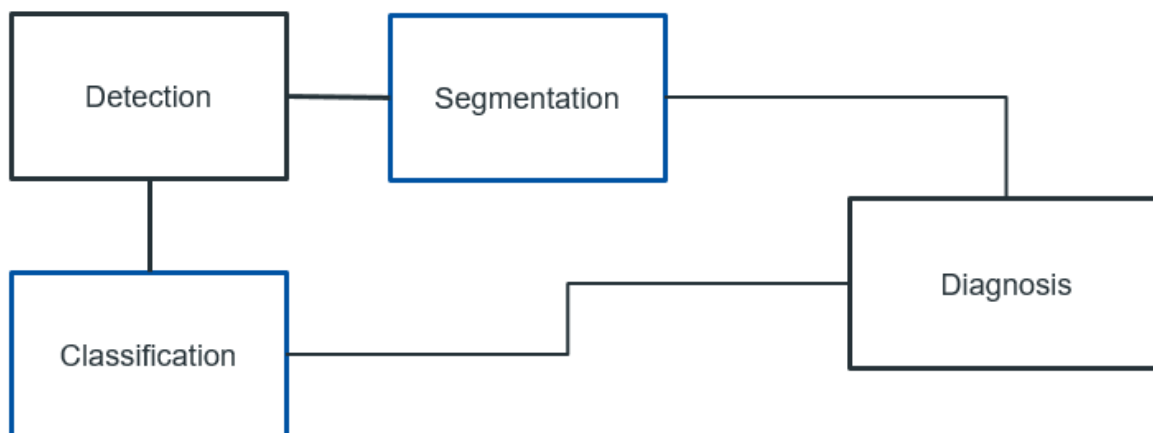


Fig.1 Steps of program



Dataset – Detection

It might go without saying that you cannot do data science without data. We could lose hundreds of pages pondering what precisely constitutes data, but for now, we will err on the practical side and focus on the key properties to be concerned with. Generally, we are concerned with a collection of examples. In order to work with data usefully, we typically need to come up with a suitable numerical representation. Each example (or data point, data instance, sample) typically consists of a set of attributes called features (or covariates), from which the model must make its predictions. In the supervised learning problems above, the thing to predict is a special attribute that is designated as the label (or target).

If we were working with image data, each individual photograph might constitute an example, each represented by an ordered list of numerical values corresponding to the brightness of each pixel. A 200×200 color photograph would consist of $200 \times 200 \times 3 = 120000$ numerical values, corresponding to the brightness of the red, green, and blue channels for each spatial location. In another traditional task, we might try to predict whether or not a patient will survive, given a standard set of features such as age, vital signs, and diagnoses.

When every example is characterized by the same number of numerical values, we say that the data consist of fixed-length vectors and we describe the constant length of the vectors as the dimensionality of the data. As you might imagine, fixed-length can be a convenient property. If we wanted to train a model to recognize cancer in microscopy images, fixed-length inputs mean we have one less thing to worry about.

Generally, the more data we have, the easier our job becomes. When we have more data, we can train more powerful models and rely less heavily on pre-conceived assumptions. The regime change from (comparatively) small to big data is a major contributor to the success of modern deep learning. To drive the point home, many of the most exciting models in deep learning do not work without large datasets. Some others work in the small data regime, but are no better than traditional approaches.

Finally, it is not enough to have lots of data and to process it cleverly. We need the right data. If the data are full of mistakes, or if the chosen features are not predictive of the target quantity of interest, learning is going to fail. The situation is captured well by the cliché: garbage in, garbage out. Moreover, poor predictive performance is not the only potential consequence. In sensitive applications of machine learning, like predictive policing, resume screening, and risk models used for lending, we must be especially alert to the consequences of garbage data. One common failure mode occurs in datasets where some groups of people are unrepresented in the training data. Imagine applying a skin cancer recognition system in the wild that had





never seen black skin before. Failure can also occur when the data do not merely under-represent some groups but reflect societal prejudices. For example, if past hiring decisions are used to train a predictive model that will be used to screen resumes, then machine learning models could inadvertently capture and automate historical injustices. Note that this can all happen without the data scientist actively conspiring, or even being aware.

In our research we used dataset detection for uterine fibroids. The task chosen for experimenting Transfer Learning consists of the classification of fibroid images into 3 different categories. The choice of this task is mainly due to the easy availability of a myomas dataset, as well as to the domain of the problem, which is generic enough to be suitable for effectively applying Transfer Learning with neural networks. After detection program will send the result for next step CNN. Depending on whether we are handling black-and-white or color images, each pixel location might be associated with either one or multiple numerical values, respectively. Until now, our way of dealing with this rich structure was deeply unsatisfying. We simply discarded each image's spatial structure by flattening them into one-dimensional vectors, feeding them through a fully-connected MLP. Because these networks are invariant to the order of the features, we could get similar results regardless of whether we preserve an order corresponding to the spatial structure of the pixels or if we permute the columns of our design matrix before fitting the MLP's parameters. Preferably, we would leverage our prior knowledge that nearby pixels are typically related to each other, to build efficient models for learning from image data. The convolutional neural networks (CNNs), a powerful family of neural networks that are designed for precisely this purpose. CNN-based architectures are now ubiquitous in the field of computer vision, and have become so dominant that hardly anyone today would develop a commercial application or enter a competition related to image recognition, object detection, or semantic segmentation, without building off of this approach.

Modern CNNs, as they are called colloquially owe their design to inspirations from biology, group theory, and a healthy dose of experimental tinkering. In addition to their sample efficiency in achieving accurate models, CNNs tend to be computationally efficient, both because they require fewer parameters than fully-connected architectures and because convolutions are easy to parallelize across GPU cores. Consequently, practitioners often apply CNNs whenever possible, and increasingly they have emerged as credible competitors even on tasks with a one-dimensional sequence structure, such as audio, text, and time series analysis, where recurrent neural networks are conventionally used. Some clever adaptations of CNNs have also brought them to bear on graph-structured data and in recommender systems.





The basic operations that comprise the backbone of all convolutional networks. These include the convolutional layers themselves, nitty-gritty details including padding and stride, the pooling layers used to aggregate information across adjacent spatial regions, the use of multiple channels at each layer, and a careful discussion of the structure of modern architectures.

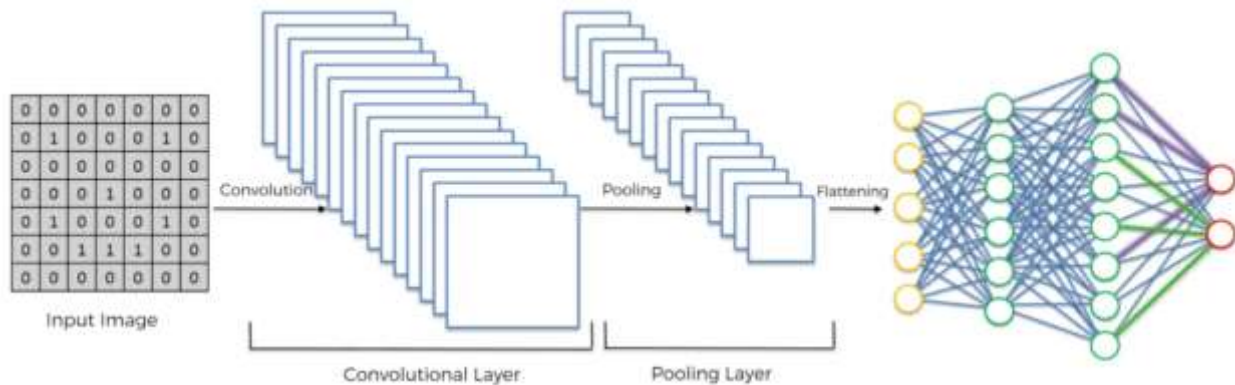


Fig.2 Convolutional neural networks (CNNs)

In this work we have some steps of CNN:

◎Convolutional Neural Network (CNN) is an neural network which extracts or identifies a feature in a particular image.

◎CNN has the following five basic components:

◎Convolution: to detect features in an image

◎ReLU: to make the image smooth and make boundaries distinct

◎Pooling: to help fix distorted images

◎Flattening: to turn the image into a suitable representation

◎Full connection: to process the data in a neural network

◎A CNN works in pretty much the same way an ANN works but since we are dealing with images, a CNN has more layers to it than an ANN.

Also we have types of classification, here you can see given classification types of job:

Classification

○ Binary = 0 } *Uncomplicated*
○ Normal = 1 }

○ Difficult = 2 } *Complicated*



Conclusion

In this work main job is detection of uterine fibroid by using Ultrasound. Detect it by dataset after segmentation and classification by U-net optimized model patient can take a decision of myoma. In future work, we will further improve the efficiency of our method by GPU acceleration and extend SF-SSM to the segmentation of 3-D US images to improve the efficiency and effect of HIFU therapy. We also try to extend the proposed idea to other related areas, such as computer-aided design, computer graphics and natural image manipulation.

References

1. E.A. Stewart Uterine Fibroids Lancet, 357 (2001), pp. 293-298 W.
2. Wang, Y. Wang, T. Wang, J. Wang, L. Wang, J. Tang Safety and efficacy of US-guided high-intensity focused ultrasound for treatment of submucosal fibroids Eur Radiol, 22 (2012), pp. 2553-2558
3. Y.-S. Kim, J.-H. Kim, H. Rhim, H.K. Lim, B. Keserci, D.-S. Bae, et al. Volumetric MR-guided high-intensity focused ultrasound ablation with a one-layer strategy to treat large uterine fibroids: initial clinical outcomes Radiology, 263 (2012), pp. 600-609
4. K. Saini, M. Dewal, M. Rohit Ultrasound imaging and image segmentation in the area of ultrasound: a review Int J Adv Sci Technol, 24 (2010)
5. S. Sridevi, M. Sundaresan Survey of image segmentation algorithms on ultrasound medical images International conference on pattern recognition, informatics and mobile engineering (PRIME), IEEE (2013), pp. 215-220
6. M. Kass, A. Witkin, D. Terzopoulos Snakes active contour models Int J Comput Vis, 1 (1988), pp. 321-331 C. Xu, J.L. Prince Snakes, shapes, and gradient vector flow IEEE Trans Image Process, 7 (1998), pp. 359-369
7. T. McInerney, D. Terzopoulos Topology adaptive snakes Med Image Anal, 4 (2000), pp. 73-91
8. Y. Wu, Y. Wang, Y. Jia Adaptive diffusion flow active contours for image segmentation Comput Vis Image Understand, 117 (2013), pp. 1421-1435
9. R. Malladi, J.A. Sethian, B.C. Vemuri Shape modeling with front propagation: a level set approach IEEE Trans Pattern Anal Mach Intell, 17 (1995), pp. 158-175
10. V. Caselles, R. Kimmel, G. Sapiro Geodesic active contours Int J Comput Vis, 22 (1997), pp. 61-79
11. N. Paragios A level set approach for shape-driven segmentation and tracking of the left ventricle IEEE Trans Med Imaging, 22 (2003), pp. 773-776





15. O. Michailovich, A. Tannenbaum Segmentation of medical ultrasound images using active contours IEEE international conference on image processing (ICIP), vol. 5, IEEE (2007), p. V-513
16. T.F. Chan, L.A. Vese Active contours without edges IEEE Trans Image Process, 10 (2001), pp. 266-277
17. S. Lankton, A. Tannenbaum Localizing region-based active contours IEEE Trans Image Process, 17 (2008), pp. 2029-2039
18. C. Li, R. Huang, Z. Ding, J. Gatenby, D.N. Metaxas, J.C. Gore A level set method for image segmentation in the presence of intensity inhomogeneities with application to MRI IEEE Trans Image Process, 20 (2011), pp. 2007-2016
19. Y. Gao, S. Bouix, M. Shenton, A. Tannenbaum Sparse texture active contour IEEE Trans Image Process, 22 (2013), pp. 3866-3878
20. L. Wang, C. Pan Robust level set image segmentation via a local correntropy-based k-means clustering Pattern Recognit, 47 (2014), pp. 1917-1925
21. Hafiane, P. Vieyres, A. Delbos Phase-based probabilistic active contour for nerve detection in ultrasound images for regional anesthesia Comput Biol Med, 52 (2014), pp. 88-95
22. Cohen, E. Rivlin, I. Shimshoni, E. Sabo Memory based active contour algorithm using pixel-level classified images for colon crypt segmentation Comput Med Imaging Graph (2015)
23. T.F. Cootes, C.J. Taylor 'Active shape models' – smart snakes Proceedings of the British machine vision conference (1992), pp. 266-275
24. G. Jacob, J.A. Noble, C. Behrenbruch, A.D. Kelion, A.P. Banning A shape-space-based approach to tracking myocardial borders and quantifying regional left-ventricular function applied in echocardiography IEEE Trans Med Imaging, 21 (2002), pp. 226-238
25. Van Ginneken, A.F. Frangi, J.J. Staal, B.M. ter Haar Romeny, M.A. Viergever Active shape model segmentation with optimal features IEEE Trans Med Imaging, 21 (2002), pp. 924-933
26. Shen, Y. Zhan, C. Davatzikos Segmentation of prostate boundaries from ultrasound images using statistical shape model IEEE Trans Med Imaging, 22 (2003), pp. 539-551
27. N. Houhou, A. Lemkaddem, V. Duay, A. Alla, J. Thiran Shape prior based on statistical map for active contour segmentation IEEE international conference on image processing (ICIP), IEEE (2008), pp. 2284-2287
28. T.F. Cootes, C.J. Taylor, D.H. Cooper, J. Graham Active shape models – their training and application Comput Vis Image Understand, 61 (1995), pp. 38-59





29. S. Wold, K. Esbensen, P. Geladi Principal component analysis Chemom Intell Lab Syst, 2 (1987), pp. 37-52
30. Cremers, F.R. Schmidt, F. Barthel Shape priors in variational image segmentation: convexity, Lipschitz continuity and globally optimal solutions IEEE conference on computer vision and pattern recognition (CVPR), IEEE (2008), pp. 1-6
31. J.B. Tenenbaum, V. De Silva, J.C. Langford A global geometric framework for nonlinear dimensionality reduction Science, 290 (2000), pp. 2319-2323
32. P. Etyngier, F. Segonne, R. Keriven Shape priors using manifold learning techniques
33. IEEE international conference on computer vision (ICCV), IEEE (2007), pp. 1-8
34. P. Yan, S. Xu, B. Turkbey, J. Kruecker Adaptively learning local shape statistics for prostate segmentation in ultrasound IEEE Trans Biomed Eng, 58 (2011), pp. 633-641
35. X. Zhou, X. Huang, J.S. Duncan, W. Yu Active contours with group similarity
36. IEEE conference on computer vision and pattern recognition (CVPR), IEEE (2013), pp. 2969-2976
37. W. Wang, L. Zhu, J. Qin, Y.-P. Chui, B.N. Li, P.-A. Heng Multiscale geodesic active contours for ultrasound image segmentation using speckle reducing anisotropic diffusion Opt Lasers Eng, 54 (2014), pp. 105-116
38. X. Liao, Z. Yuan, Q. Zheng, Q. Yin, D. Zhang, J. Zhao Multi-scale and shape constrained localized region-based active contour segmentation of uterine fibroid ultrasound images in HIFU therapy PLOS ONE, 9 (2014), p. e103334
39. X. Huang, D.P. Dione, C.B. Compas, X. Papademetris, B.A. Lin, A. Bregasi, et al.
40. Contour tracking in echocardiographic sequences via sparse representation and dictionary learning Med Image Anal, 18 (2014), pp. 253-271
41. X. Qin, Y. Tian, P. Yan Feature competition and partial sparse shape modeling for cardiac image sequences segmentation Neurocomputing, 149 (2015), pp. 904-913
42. Y. Zhu, X. Papademetris, A.J. Sinusas, J.S. Duncan A dynamical shape prior for LV segmentation from RT3D echocardiography Medical image computing and computer-assisted intervention – MICCAI 2009, Springer (2009), pp. 206-213
43. C. Garnier, J.-J. Bellanger, K. Wu, H. Shu, N. Costet, R. Mathieu, et al.
44. Prostate segmentation in HIFU therapy IEEE Trans Med Imaging, 30 (2011), pp. 792-803
45. T. Shepherd, S.J. Prince, D.C. Alexander Interactive lesion segmentation with shape priors from offline and online learning IEEE Trans Med Imaging, 31 (2012), pp. 1698-1712





46. C. Cengizler, M. Guven, M. Avci A fluid dynamics-based deformable model for segmentation of cervical cell images *Signal Image Video Process*, 8 (2014), pp. 21-32
47. X. Yuan, F. Zhong, Y. Zhang, Q. Peng Automatic segmentation of head-and-shoulder images by combining edge feature and shape prior *International conference on computer-aided design and computer graphics (CAD/graphics)*, IEEE (2011), pp. 163-170
48. C.W. Gardiner *Handbook of stochastic methods*, vol. 3, Springer, Berlin (1985)
49. H. Risken *The Fokker–Planck equation: methods of solution and applications*
50. Springer Verlag (1985)
51. T. Frank, P. Beek, R. Friedrich Fokker–Planck perspective on stochastic delay systems: exact solutions and data analysis of biological systems *Phys Rev E*, 68 (2003), p. 021912
52. R. Friedrich, S. Siegert, J. Peinke, S. Lück, M. Siefert, M. Lindemann, et al. Extracting model equations from experimental data *Phys Lett A*, 271 (2000), pp. 217-222
53. Sarti, C. Corsi, E. Mazzini, C. Lamberti Maximum likelihood segmentation of ultrasound images with Rayleigh distribution *IEEE Trans Ultrason Ferroelectr Freq Control*, 52 (2005), pp. 947-960
54. Boukerroui A local Rayleigh model with spatial scale selection for ultrasound image segmentation *British machine vision conference* (2012)
55. J.K. Udupa, V.R. LaBlanc, H. Schmidt, C. Imielinska, P.K. Saha, G.J. Grevera, et al.
56. Methodology for evaluating image-segmentation algorithms *Medical imaging. International society for optics and photonics* (2002), pp. 266-277
57. B. Sahiner, N. Petrick, H.-P. Chan, L.M. Hadjiiski, C. Paramagul, M.A. Helvie, et al.
58. Computer-aided characterization of mammographic masses: accuracy of mass segmentation and its effects on characterization *IEEE Trans Med Imaging*, 20 (2001), pp. 1275-1284
59. D.P. Huttenlocher, G.A. Klanderman, W.J. Rucklidge Comparing images using the Hausdorff distance *IEEE Trans Pattern Anal Mach Intell*, 15 (1993), pp. 850-863
60. C. Li, C. Xu, C. Gui, M.D. Fox Distance regularized level set evolution and its application to image segmentation *IEEE Trans Image Process*, 19 (2010), pp. 3243-3254
61. M. Yang, Y. Yuan, X. Li, P. Yan Medical image segmentation using descriptive image features *British machine vision conference* (2011), pp. 1-11





62. X. Cai, F. He, W. Li, X. Li, Y. Wu Encryption based partial sharing of CAD models
63. *Integr Comput-Aid E*, 22 (2015), pp. 243-260
64. H. Liu, F. He, F. Zhu, Q. Zhu Real time control of human actions with inertial sensors
65. *Sci China Ser F*, 57 (2014), pp. 072113:1-072113:11
66. X. Li, F. He, X. Cai, D. Zhang, Y. Chen A method for topological entity matching in the integration of heterogeneous CAD systems *Integr Comput-Aid E*, 20 (2014), pp. 15-30
67. Y. Cheng, F. He, X. Cai, D. Zhang A group undo/redo method in 3D collaborative modeling systems with performance evaluation *J Newt Comput Appl*, 36 (2013), pp. 1512-1522
68. H. Liu, F. He, X. Cai, X. Chen Performance-based Control Interfaces using mixture of factor analyzers *Visual Comput*, 27 (2011), pp. 595-603
69. Z. Huang, F. He, X. Cai, Z. Zou, J. Liu, M. Liang, et al. Efficient random saliency map detection *Sci China Ser F*, 54 (2011), pp. 1207-1217
70. S. Jing, F. He, S. Han, X. Cai, H. Liu A method for topological entity correspondence in a replicated collaborative CAD system *Comput Ind*, 60 (2009), pp. 467-475

